PROCEEDINGS, 50th Workshop on Geothermal Reservoir Engineering
Stanford University, Stanford, California, February 10-12, 2025
SGP-TR-229

Impacts of Vertical-fracture Networks on Enhanced Geothermal Systems

Zhenqian Xue[1], and Zhangxing Chen[1]

[1]University of Calgary, 2500 University Drive NW, Calgary, Alberta, Canada T2N 1N4

zhenqian.xue@ucalgary.ca

Keywords: Enhanced geothermal systems, Vertical-fracture networks, THMC, Well dynamics

ABSTRACT

Hot dry rock (HDR) fracturing is a critical stage in the development of enhanced geothermal systems (EGS). Vertical-fracture network, as a widely applied fracture system, its properties and morphology significantly affect heat extraction performance. However, current studies exploring the effect of various fracture networks often lack completeness and accuracy, where chemical reactions, wellbore dynamic, and/or rock mechanical behaviors are overlooked. In this study, combined thermal-hydraulic-mechanical-chemical (THMC) and wellbore heat loss models are developed to investigate EGS heat recovery under different vertical-fracture patterns. The impacts of fracture properties on heat mining are also determined. The results from the proposed combined EGS models indicate that EGS heat recovery improves with increasing fracture spacing, fracture number, and decreasing fracture conductivity, but the performance gains diminish as spacing, and number increase further. Meanwhile, excessively low fracture conductivity may lead to ineffective fluid flow in the reservoir. Therefore, an effective design of these parameters is critical in the HDR stimulation process. Additionally, the interrupted complex fracture network demonstrates the highest power and electricity generation. Although interrupted fractures require higher injection pressure, this is effectively offset by the complex fracture pattern, resulting in a similar injection-production pressure difference to that of the continuous simple fracture network. Therefore, interrupted complex fracture networks are recommended when a vertical-fracture network is determined to be created. This study accurately improves the understanding of EGS performance under different vertical-fracture networks, offering operators valuable insights to improve decision-making in EGS development.

1. INTRODUCTION

Geothermal energy has stand out as a highly attractive renewable resource in the fight against climate change, with promising potential to support the transition to clean energy. Its benefits extends beyond electricity generation, heating and cooling, energy storage, and carbon capture (Xue & Chen, 2023). In particular, enhanced geothermal systems (EGS) are widely acknowledged as the most promising for providing sustainable and low-carbon energy for electricity generation and residential heating and cooling (Lu, 2018). Recognizing the critical role of EGS in the energy transition, many countries are prioritizing its development. For example, the United States has highlighted the Enhanced Geothermal Shot as a critical initiative toward achieving 100% carbon-free electricity and net-zero emissions.

EGS development represents the energy extraction from hot dry rock (HDR), which typically requires initial stimulation because HDR is impermeable (Sowiżdżał et al., 2022). HDR stimulation is used to create high-conductivity zones that facilitate fluid flow and heat transfer. In current EGS projects, stimulation methods such as hydraulic fracturing, thermally-induced fracturing, and chemical stimulation have been successfully utilized (Charlez et al., 1996). Different fracturing methods are possible to induce various fracture patterns in HDR reservoirs. For example, hydraulic fracturing typically generates simple vertical-fracture patterns, where only primary pathways are formed to connect injection and production wells and may require proppants to keep the fractures open (Li et al., 2022). In contrast, thermally-induced fracturing is often operated in the reservoirs with abundant nature fractures. This method tends to create a shear-fracture network by reactivating and cleaning existing fractures, reopening them without creating new ones (Siratovich et al., 2011). Currently, hydraulic fracturing is the most applied, which requires high treatment pressures to establish fractures in the reservoir. The feasibility of vertical-fracture networks on extracting effective heat energy has been proven (Hofmann et al., 2016). In addition, CO_2 fracturing, which has been highly effective in unconventional oil and gas reservoirs (Ma et al., 2022; Song et al., 2019; Xue et al., 2024), shows potential for HDR applications (Borgia et al., 2013; Zhang et al., 2021). Although large-scale field operations using CO_2 to stimulate HDR reservoirs have not yet been conducted, it has been suggested that CO_2 fracturing could create complex and branched vertical-fracture networks in granite based on previous mesoscale experiments and numerical simulations (Feng et al., 2021; Hou et al., 2021; Isaka et al., 2019).

Understanding the heat extraction performance under various fracture networks is crucial due to their significant influence on overall heat mining efficiency (Liao et al., 2023). However, EGS development is a complex process, involving multiple subsurface interactions such as heat transfer, fluid flow, mechanical deformation, and chemical reactions, as well as heat loss in wellbores during fluid injecting and lifting (Gan et al., 2021; Xie et al., 2025). Previous studies have developed reservoir models to simulate different vertical-fracture configurations in HDR reservoirs, aiming to understand the relationship between fracture complexity and heat recovery (Shi et al., 2019). For example, Ma et al. (2020) and Slatlem Vik et al. (2018) investigated the influence of fracture number and fracture spacing respectively on heat recovery with considering the mechanisms of heat transfer and fluid flow. Aliyu et al. (2021) also generated thermal-hydraulic (TH) modeling and determined the critical role of fracture permeability variations in improving HDR geothermal reservoir performance. In addition, Shi et al. (2019) and Liu et al. (2023) developed thermal-hydraulic-mechanical (THM) models to simplify fracture systems and analyzed the effects of fracture network geometries on heat extraction efficiency. However, some critical behaviors are overlooked

in these models, such as chemical reactions and wellbore dynamics. Without a comprehensive consideration of different mechanisms, the evaluation of an EGS development often lack completeness and accuracy.

To the best of our knowledge, the current understanding of EGS heat extraction efficiency under different vertical-fracture networks still remains incomplete for operators. In specific, a fully coupled model that integrates thermal, hydraulic, mechanical, and chemical processes has not been considered in studying the impact of various fracture networks on heat recovery. Previous works normally neglect mechanical or chemical behaviors in their models. In addition, heat loss in the wellbore, a critical factor in deep HDR reservoirs, has not been considered in current studies. This study aims to address these gaps by developing advanced EGS reservoir models that fully integrate THMC behaviors and wellbore heat loss during EGS development. These models are used to investigate the effects of different vertical-fracture networks and the influence of various fracture properties on geothermal energy production. By providing a more detailed understanding of complex subsurface interactions and wellbore dynamics, this work offers valuable practical insights for operators and supports informed decision-making regarding fracturing technologies, optimizing heat recovery strategies, and improving the overall feasibility and efficiency of EGS development.

2. METHODOLOGY

In this study, CMG-STARS software is utilized to generate reservoir models for characterizing complex reservoir interactions and wellbore dynamics and for investigating the impact of vertical-fracture networks on heat recovery. To simplify the numerical models, the following reasonable assumptions are made: (1) The formation properties are homogeneous and isotropic; (2) The reservoir is initially saturated with water; (3) Water is the only flow medium, with properties that vary based on temperature and pressure; (4) Local thermal equilibrium is assumed, meaning no temperature difference exists between the fluid and rock at the same location; and (5) Amorphous silica is the primary mineral involved in chemical reactions, and the relevant solid or mineral reaction is: $SiO_{2(s)} + 2H_2O \leftrightarrow H_4SiO_4$. The reservoir models created in this study are based on our previous models of the Qiabuqia EGS (Xue et al., 2023; 2024; 2024; 2023; 2023)The details about the Qiabuqia field can be found in previous studies (Lei et al., 2019, 2020). A base model is first developed to represent an area of 1500 × 1500 × 3800 m^3 with a total of 34,200 grid blocks. The key reservoir properties of this model can be found in Table 1.

Table 1: Reservoir properties in reservoir models.

Parameter	Value	Parameter	Value
Granite density, kg/m^3	44	Granite heat conductivity, W/(m·℃)	3.0
Porosity, %	45	Granite specific heat, J/(kg·℃)	980
Temperature, ℃	25-0.057z	Thermal expansion coefficient (℃$^{-1}$)	7.5×10^{-6}
Pressure, MPa	0.1-0.01z	Biot's coefficient	0.7
Horizontal permeability, mD	0.26	Young's modulus (GPa)	44.1
Vertical permeability, mD	0.026	Poisson's ratio	0.23
Sillica initial volume fraction	0.45	Horizontal and vertical natural fracture spacing, m	10

In this model, three horizontal wells (one injection well and two production wells) are drilled at a depth of 3,700 m, with a well spacing of 500 m and a horizontal length of 750 m. The engineered fractures in this base model are represented by a simple vertical-fracture network, consisting of six planar fractures with a spacing of 150 m, a half-length of 500 m, and a conductivity of 10 mDm, connecting the injector to the producers. To ensure accurate calculations, the grid resolution in the enhanced reservoir is refined five times horizontally and three times vertically. Regarding the complex subsurface mechanisms, porosity change is determined as the coupling node to characterize the interactions between fluid flow, heat transfer, geomechanical deformation, and chemical reactions in the reservoir. For the boundary conditions, fluid flow is restricted at both the top and bottom boundaries of the model. The temperature at the bottom boundary is set based on the temperature distribution observed in the Qiabuqia field. At the top boundary, a heat loss model is implemented to simulate the heat losses from the surface to the atmosphere. For the initial conditions, based on the exploration data from this field, the temperature and pressure at the top of the study area are set to 236°C and 37.1 MPa, respectively. Figure 1 provides a schematic diagram of this base model and demonstrates the mechanisms of underground interactions and wellbore heat loss.

In terms of wellbore dynamics, the heat loss and pressure drop during fluid injecting and lifting are analyzed by using the Semi-Analytical Model (SAM) in CMG-STARS software. The wellbore model is designed by dividing the vertical section of each well into 150 equal segments. The lengths of the casing and insulation are both set to match the wellbore depth of 3,700 m. Detailed parameter setting of the wellbore model can be found in Table 2. Water is used as the heat transmission fluid in this work, and a water stream at 40 ℃ is injected into the reservoir through the injection well. The operational constraints for the wells are as follows: the injection well operates at a constant rate of 45 kg/s, and the production wells maintain a constant pressure of 37 MPa. The system is designed for heat extraction and water circulation over a 20-year period. Detailed settings of the operating parameters for the simulation are outlined in Table 2.

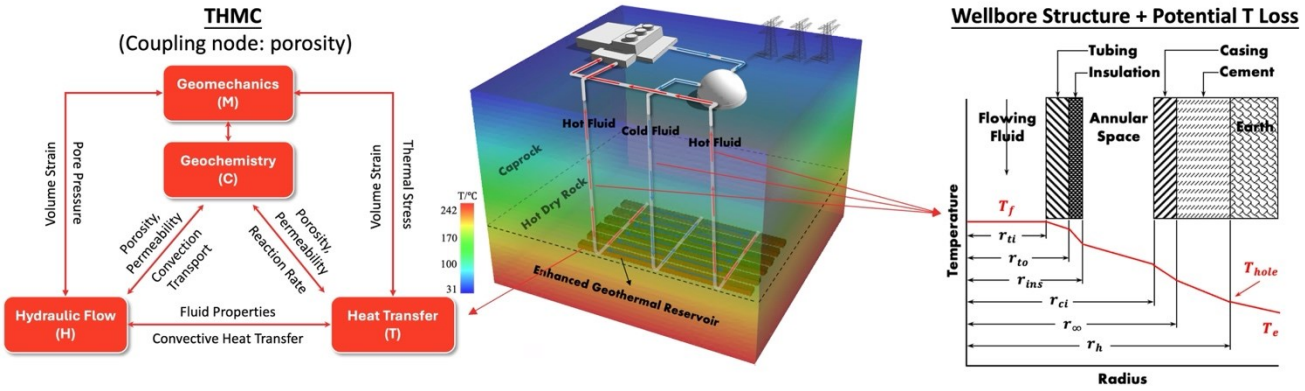

Figure 1: Schematic diagram of a horizontal-well-EGS reservoir model: (left) complex interactions in the reservoir, and (right) a wellbore structure with potential temperature loss

Table 2: Wellbore and operational properties in reservoir models.

Parameter	Value	Parameter	Value
Well depth, m	3700	Cement thermal conductivity, W/(m·°C)	0.26
Well spacing, m	500	Fracture spacing, m	150
Well horizontal section length, m	750	Fracture half-length, m	500
Inner and outer tubing radius, m	0.15, 0.18	Fracture conductivity, mDm	10
Insulation radius, m	0.2	Fracture number	6
Inner and outer casing radius, m	0.24, 0.3	Injection rate, kg/s	45
Tubing thermal conductivity, W/(m·°C)	32.29	Injection temperature, °C	40
Insulation thermal conductivity, W/(m·°C)	0.06	Production pressure, MPa	37
Casing thermal conductivity, W/(m·°C)	32.29	Operation time, year	20

In addition to the generated THMC base model, different coupling models, including TH (thermal-hydraulic), THM (thermal-hydraulic-mechanical), and THC (thermal-hydraulic-chemical), are developed to evaluate the impact of different coupling mechanisms on reservoir performance and heat recovery. The TH model considers only fluid flow and heat transfer within the matrix and fractures. The THM model adds rock deformation to the fluid flow and heat transfer processes, while the THC model incorporates chemical reactions along with fluid flow and heat transfer. The fully coupled THMC model accounts for fluid flow, heat transfer, mechanical deformation, and chemical reactions. All models include wellbore heat loss for a more accurate representation.

Based on the validated THMC model, the effects of various vertical-fracture networks and fracture properties on reservoir performance were explored. First, a sensitivity analysis is performed on various fracture properties, including fracture spacing (ranging from 50 to 200 m), fracture number (ranging from 5 to 14), and fracture conductivity (ranging from 5 to 20 mDm). Second, heat mining performance is evaluated under different vertical-fracture networks, considering simple, complex, continuous, and interrupted fracture systems, as shown in Figure 2. The detailed fracture setting in these cases are as follows: Scenario #1: Involves only primary fractures connecting the injector and producers; Scenario #2: Includes both primary fractures (500 m half-length) and secondary fractures (50 m half-length); Scenarios #3 and #4: represent interrupted simple and complex fracture networks generated with primary fractures having a half-length of 250 m and secondary fractures in the complex network measuring 50 m in length. These scenarios simplify the representation of various fracturing methods, enabling a comprehensive analysis of their impact on heat recovery and reservoir performance.

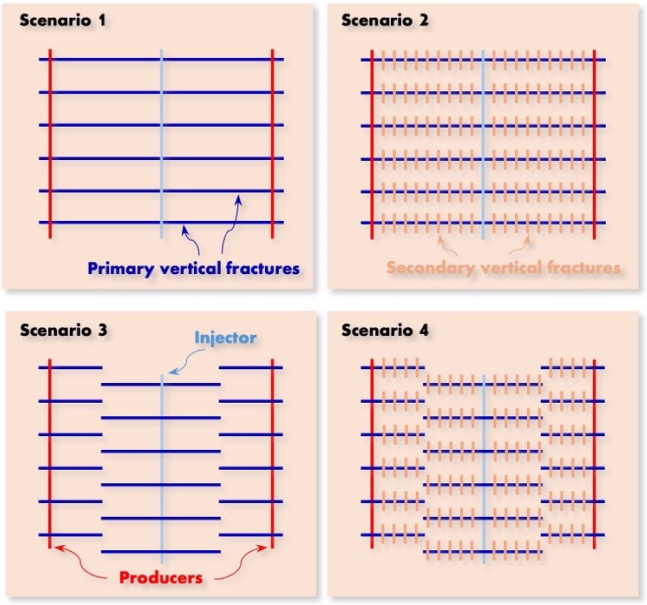

Figure 2: Upward geometric views of scenarios with different vertical-fracture networks

To evaluate the heat extraction performance, two indicators, including the temperature of the produced fluid at the surface and geothermal electricity, are considered. The surface production temperature is directly calculated by CMG-STARS, and the generated geothermal electricity (E) is determined by the installed geothermal power capacity (W_p), which can be calculated by Equation 1 (Lei et al., 2019) and Equation 2 (Xue, 2024), respectively.

$$E = \sum_t^T W_p^t \cdot H_{annual} \cdot 0.7 \tag{1}$$

$$W_p = 0.3 \cdot Q \cdot \Delta H \cdot (1 - T_{in}/T_{out}) \tag{2}$$

Where T represents the total number of operation periods, and H_{annual} is the total number of hours in a year, which is 8760 (365 days × 24 hours). Q denotes the fluid production rate for the entire system; ΔH is the enthalpy change between the injected enthalpy and produced enthalpy; T_{in} represents the rejection temperature; T_{out} is the average temperature at the production wells. In this study, it is assumed that all produced heat is utilized for power generation, with an energy conversion efficiency of 30%, meaning 30% of the thermal energy is converted into geothermal electricity. To evaluate the reliability of the geothermal power plant, a capacity factor of 0.7 is applied.

3. RESULTS AND DISCUSSIONS

3.1 Various coupling models

Figure 3 demonstrates the porosity distributions after twenty years of operation across different coupling models, which highlight notable differences in conductivity and porosity changes due to varying interactions in the reservoir. The results indicate that the conductivity is increased near the wellbore in the THC model due to the the dissolution of silica minerals. Conversely, the THM model illustrates a longer and narrower high-conductivity area distributed along the engineered fractures, driven by mechanical deformation. By incorporating both mechanical deformation and chemical reactions in the THMC model, the porosity changes are observed to be closely resemble those of the THM model.

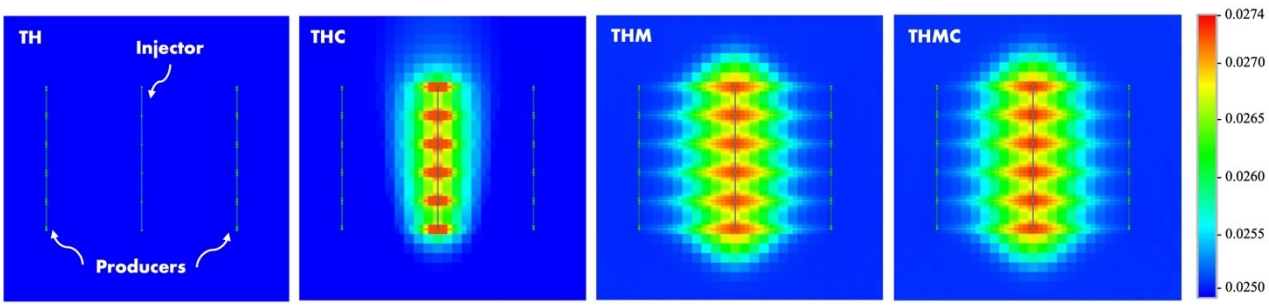

Figure 3: Porosity distributions after twenty years operation in various coupling models

Heat loss in another critical factor affecting the efficiency of heat recovery in EGS. As depicted in Figure 4, wellbore heat loss across all models is most significant during the initial stages of operation, gradually decreasing over time and stabilizing in later years. This trend occurs because the initially produced fluid, which is at a higher temperature than the surrounding formation, needs to transfer heat to the formation until thermal equilibrium is reached. In addition, the THC model presents the lowest temperature loss in wellbores, attributed to its higher water production rate. Conversely, the THM model demonstrates the largest temperature loss due to the fact that more enthalpy and geothermal energy are carried in higher flow rates, which facilitates heat transfer while minimizes the temperature difference between the wellbore and the surrounding formation (Xie et al., 2025).

The variances in petrophysical parameters and wellbore heat loss help explain the differences in heat extraction performance among the models. All subsequent comparisons are conducted relative to the TH model. For example, according to Figure 4, the increased porosity and permeability along the flow path in the THM model result in higher flow rates within the reservoir. This leads to greater heat loss in the wellbore and a more rapid decline in production temperature, ultimately causing smaller geothermal power and electricity output. In contrast, the THC model demonstrates improved heat mining performance, characterized by a higher surface production temperature and greater electricity generation. This is due to its increased high-conductivity zone near the wellbore, which extends the residence time of the injected cold fluid in the reservoir, delays thermal breakthrough, and minimizes wellbore heat loss. In the THMC model, combined effects of mechanical deformation and chemical reactions contributes to a higher surface production temperature and greater net power and electricity generation. These improvements are attributed to extended fluid flow times, increased production rates, and lower injection pressures.

It is important to highlight that the opposing effects of mechanical deformation and chemical reactions on production temperature and heat recovery, along with the similar reservoir performance trends observed in the THM and THMC models, are consistent with findings from previous research (Pandey et al., 2015; Salimzadeh & Nick, 2019). This consistency reinforces the validity of the base THMC model developed in this study. Consequently, the generated model offers a more comprehensive evaluation of EGS performance by accounting for complex reservoir interactions as well as heat loss in wellbores. In the following section, this model will be applied to investigate the influence of various vertical-fracture networks on EGS development.

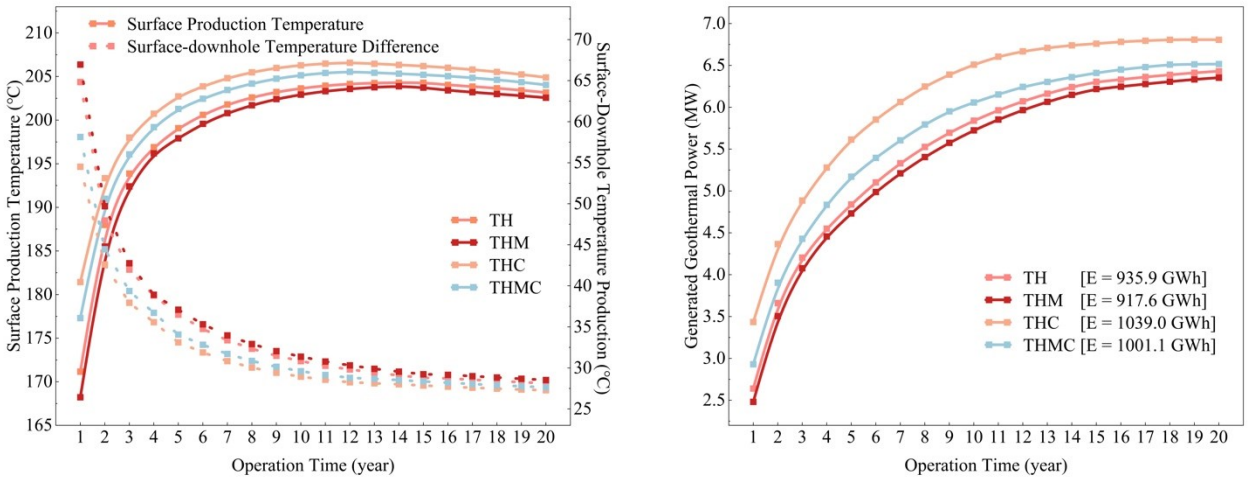

Figure 4: Surface production temperature and temperature loss within wellbores (left) and geothermal power and electricity generation (right) of different coupling models

3.2 Various fracture properties

Figures 5, 6 and 7 demonstrate the impact of different fracture spacings, numbers, and conductivity on EGS heat extraction performance, respectively. The results reveal that surface production temperature, geothermal power output, and electricity generation all increase as fracture spacing widens and the number of fractures increases. In terms of fracture spacing, these positive trends can be explained by fracture interference and the heat extraction area. Narrower fracture spacing leads to greater fracture interference and a smaller heat extraction area, resulting in higher injection pressures, faster fluid flow to the production wells, and lower surface production temperature. Consequently, this reduces geothermal power and electricity generation. For fracture number, increasing number of engineered fractures enlarges the heat extraction area, which lowers the injection pressure required to inject the same fluid volume and increases the water production rate. Additionally, the expanded heat extraction area delays the filling of fractures with injected fluid, slowing the decline in surface production temperature. As a result, the reservoirs with more engineered fractures achieve higher power and electricity generation. However, the improvement diminishes at higher fracture numbers and wider spacings as the system approaches performance saturation.

Regarding fracture conductivity, the results show an inverse relationship with overall heat mining performance, where heat recovery increases as fracture conductivity decreases. Fracture conductivity, determined by fracture permeability and aperture, significantly affects

fluid flow behavior in the reservoir. Higher fracture conductivity facilitates easier fluid flow to production wells, which accelerates thermal breakthrough and increases the decline in surface production temperature. In addition, increased fracture conductivity lowers the injection pressure under the well constraints of constant injection rate and constant production pressure. This results in smaller injection-production pressure differences and increased water production rates. However, in the cases with larger fracture conductivity, the increase in water production rate due to higher conductivity and flowability in the reservoir is counterbalanced by the reduced injection-production pressure difference, leading to minimal difference in water production rates across various fracture conductivity scenarios. Overall, the combination of reduced surface production temperature and minor differences in water production leads to lower geothermal power output and electricity generation as fracture conductivity increases.

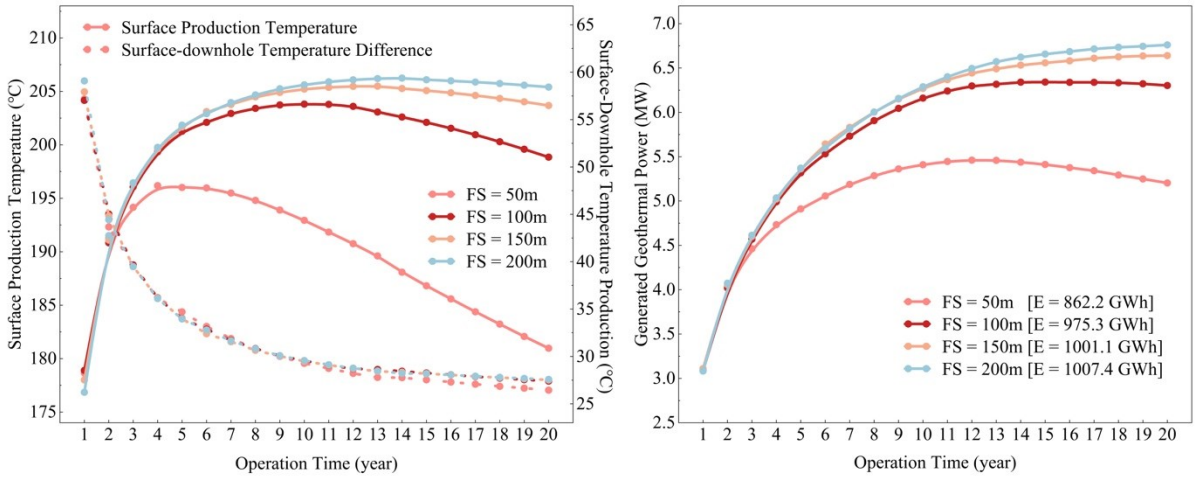

Figure 5: Surface production temperature and temperature loss within wellbores (left) and geothermal power and electricity generation (right) of different fracture spacing

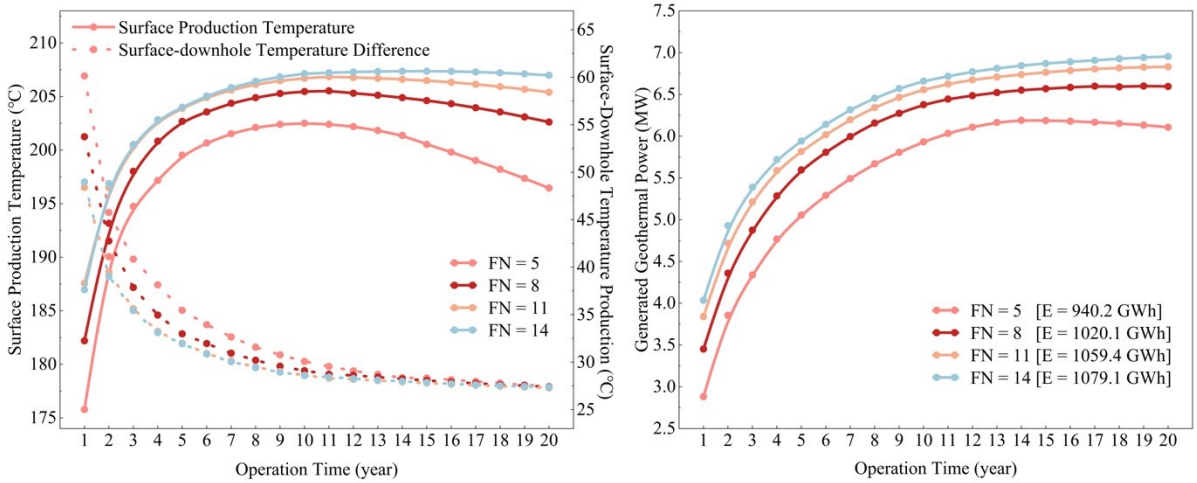

Figure 6: Surface production temperature and temperature loss within wellbores (left) and geothermal power and electricity generation (right) of different fracture number

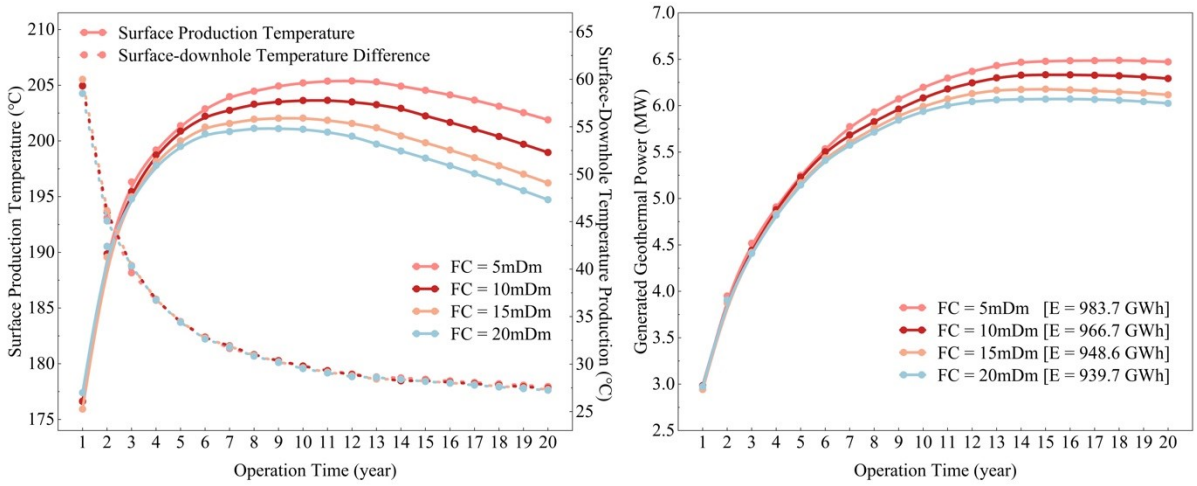

Figure 7: Surface production temperature and temperature loss within wellbores (left) and geothermal power and electricity generation (right) of different fracture conductivity

3.3 Various vertical-fracture networks

Based on the validated THMC base model, various vertical-fracture networks are applied to the Qiabuqia EGS to assess their impact on heat extraction performance, and the results are illustrated in Figure 8. The results reveal that scenario 2 achieves a higher production temperature in the surface and larger net power and electricity production compared to scenario #1. This is because the more complex vertical-fracture pattern in scenario #2, as opposed to the simpler fracture network in scenario #1. The complex fractures in scenario #2 provide a larger high-conductivity area for fluid flow and heat exchange, which slows the direct path of fluid to the production wells. Meanwhile, it also improves the flow characteristics, leading to a higher water production rate and lower temperature loss in the wellbore. Consequently, better overall heat extraction performance can be observed in scenario #2. Similarly, among interrupted vertical-fracture networks, scenario #4, which has a complex fracture pattern with larger permeable areas, shows superior heat extraction performance compared to simple fracture network (scenario #3), where scenario #4 exhibits higher surface production temperatures, greater net power, and increased electricity generation. These results are due to reduced heat loss in the wellbores, a higher water production rate, and a smaller injection-production pressure difference in the more complex fracture network.

When comparing the effects of continuous (scenarios #1 and #2) and interrupted (scenarios #3 and #4) vertical-fracture patterns, the interrupted fracture networks demonstrate higher surface production temperatures and produces more net power and further convert more electricity. This is because the absence of a direct high-conductivity pathway in interrupted networks forces the injected cold fluid to take a longer flow path to the production wells. This further results in a slower decline in production temperature and more stable geothermal power output in interrupted vertical-fracture networks. In addition, interrupted fracture networks require a higher injection pressure to inject the same amount of fluid, which increases the injection-production pressure difference and enhances the water mass flow rate. The combination of improved flow rate and stable production temperature make interrupted vertical-fracture patterns more effective for heat extraction.

The findings suggest that complex fracture networks are advantageous for sustainable heat extraction and cumulative heat recovery, where networks with more secondary, branched, and interrupted fractures are preferred over simple and continuous fracture patterns. However, the higher injection pressure required for interrupted fracture patterns may induce challenges for field operation. To mitigate this, branched fractures, which enhance subsurface conductivity and injectivity, are recommended to reduce injection pressure requirements. Therefore, HDR stimulation operations are recommended to be conducted at both the injection and production wells to generate interrupted vertical-fracture networks. Techniques such as CO_2 fracturing are preferred over hydraulic fracturing because this method are more effective in creating complex fracture patterns and reducing injection pressure requirement. If the reservoir contains pre-existing nature fractures, stimulation should aim to create vertical fractures that can connect as many of these nature fractures as possible to form a complex fracture system in the reservoir. However, in reservoirs with abundant natural fractures, further evaluation is necessary to compare heat recovery performance between vertical-fracture and shear-fracture networks before finalizing the stimulation strategy.

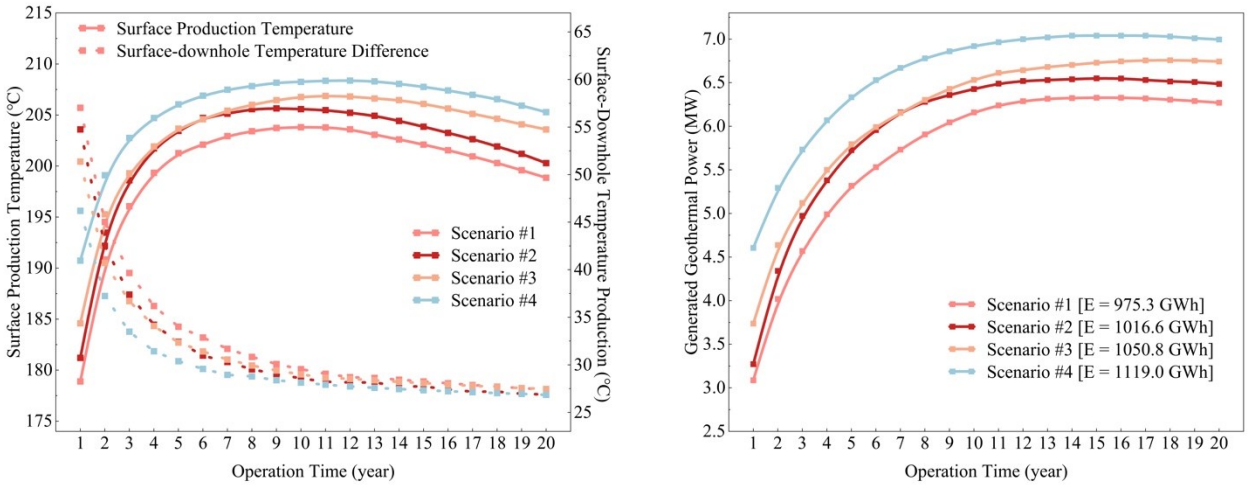

Figure 8: Surface production temperature and temperature loss within wellbores (left) and geothermal power and electricity generation (right) of different vertical-fracture networks

4. CONCLUSION

This study develops advanced EGS reservoir models that incorporate complex subsurface mechanisms and wellbore heat loss to analyze the impact of various fracture networks on heat extraction performance. By integrating thermal processes, fluid flow, mechanical deformation, chemical reactions, and wellbore heat loss, the proposed coupled models provide a more precise characterization of EGS heat recovery, which captures both detailed variations in reservoir performance and wellbore dynamics during fluid injection and extraction.

In vertical-fracture systems, EGS heat recovery improves with wider fracture spacing, a greater number of fractures, and lower fracture conductivity. However, the performance gains taper off as fracture spacing and number continue to increase. Furthermore, excessively low fracture conductivity is possible to induce insufficient heat extraction rate, reducing overall efficiency. Therefore, it is crucial to conduct an effective fracturing optimization on these parameters in the HDR stimulation process.

For various fracture patterns, interrupted fracture networks demonstrate higher power output and electricity generation than continuous fracture patterns, and meanwhile complex fracture networks perform better in overall heat extraction performance compared to simple fracture networks. Although interrupted fracture patterns require higher injection pressure, the complex fracture geometry compensates for this by maintaining a comparable injection-production pressure difference to that of simpler, continuous fracture networks. As a result, interrupted and complex vertical-fracture networks are recommended when vertical fractures are determined to be created.

This work delivers a comprehensive and accurate assessment of EGS performance, offering valuable guidance for HDR fracturing strategies and heat extraction operations. However, given that thermally-induced fracturing is also employed in EGS reservoirs, further investigation is needed to evaluate the performance of shear fracture networks. Future studies should compare the effectiveness of shear-fracture and vertical-fracture patterns to enhance decision-making efficiency and optimize EGS development strategies.

REFERENCES

Aliyu, M. D., & Archer, R. A. (2021). Numerical simulation of multifracture HDR geothermal reservoirs. *Renewable Energy*, *164*, 541–555.

Borgia, A., Pruess, K., Kneafsey, T. J., Oldenburg, C. M., & Pan, L. (2013). Simulation of CO2-EGS in a Fractured Reservoir with Salt Precipitation. *Energy Procedia*, *37*, 6617–6624.

Charlez, P., Lemonnier, P., Ruffet, C., Bouteca, M. J., & Tan, C. (1996). *Thermally induced fracturing: Analysis of a field case in north sea*. SPE-36916-MS.

Feng, C., Wang, H., & Jing, Z. (2021). Investigation of heat extraction with flowing CO2 from hot dry rock by numerical study. *Renewable Energy*, *169*, 242–253.

Gan, Q., Candela, T., Wassing, B., Wasch, L., Liu, J., & Elsworth, D. (2021). The use of supercritical CO2 in deep geothermal reservoirs as a working fluid: Insights from coupled THMC modeling. *International Journal of Rock Mechanics and Mining Sciences*, *147*, 104872.

Hofmann, H., Babadagli, T., Yoon, J. S., Blöcher, G., & Zimmermann, G. (2016). A hybrid discrete/finite element modeling study of complex hydraulic fracture development for enhanced geothermal systems (EGS) in granitic basements. *Geothermics*, *64*, 362–381.

Hou, L., Zhang, S., Elsworth, D., Liu, H., Sun, B., & Geng, X. (2021). Review of fundamental studies of CO2 fracturing: Fracture propagation, propping and permeating. *Journal of Petroleum Science and Engineering*, *205*, 108823.

Isaka, B. L. A., Ranjith, P. G., Rathnaweera, T. D., Perera, M. S. A., & Kumari, W. G. P. (2019). Influence of long-term operation of supercritical carbon dioxide based enhanced geothermal system on mineralogical and microstructurally-induced mechanical alteration of surrounding rock mass. *Renewable Energy*, *136*, 428–441.

Lei, Z., Zhang, Y., Yu, Z., Hu, Z., Li, L., Zhang, S., Fu, L., Zhou, L., & Xie, Y. (2019). Exploratory research into the enhanced geothermal system power generation project: The Qiabuqia geothermal field, Northwest China. *Renewable Energy*, *139*, 52–70.

Lei, Z., Zhang, Y., Zhang, S., Fu, L., Hu, Z., Yu, Z., Li, L., & Zhou, J. (2020). Electricity generation from a three-horizontal-well enhanced geothermal system in the Qiabuqia geothermal field, China: Slickwater fracturing treatments for different reservoir scenarios. *Renewable Energy*, *145*, 65–83.

Li, S., Wang, S., & Tang, H. (2022). Stimulation mechanism and design of enhanced geothermal systems: A comprehensive review. *Renewable and Sustainable Energy Reviews*, *155*, 111914.

Liao, J., Hu, K., Mehmood, F., Xu, B., Teng, Y., Wang, H., Hou, Z., & Xie, Y. (2023). Embedded discrete fracture network method for numerical estimation of long-term performance of CO2-EGS under THM coupled framework. *Energy*, *285*, 128734.

Liu, G., Yuan, Z., Zhou, C., Fu, Z., Rao, Z., & Liao, S. (2023). Heat extraction of enhanced geothermal system: Impacts of fracture topological complexities. *Applied Thermal Engineering*, *219*, 119236.

Lu, S.-M. (2018). A global review of enhanced geothermal system (EGS). *Renewable and Sustainable Energy Reviews*, *81*, 2902–2921.

Ma, D., Duan, H., Zhang, Q., Zhang, J., Li, W., Zhou, Z., & Liu, W. (2020). A numerical gas fracturing model of coupled thermal, flowing and mechanical effects. *Computers, Materials & Continua*, *65*(3), 2123–2141.

Ma, H., Yang, Y., Zhang, Y., Li, Z., Zhang, K., Xue, Z., Zhan, J., & Chen, Z. (2022). Optimized schemes of enhanced shale gas recovery by CO2-N2 mixtures associated with CO2 sequestration. *Energy Conversion and Management*, *268*, 116062.

Pandey, S. N., Chaudhuri, A., Rajaram, H., & Kelkar, S. (2015). Fracture transmissivity evolution due to silica dissolution/precipitation during geothermal heat extraction. *Geothermics*, *57*, 111–126.

Salimzadeh, S., & Nick, H. M. (2019). A coupled model for reactive flow through deformable fractures in Enhanced Geothermal Systems. *Geothermics*, *81*, 88–100.

Shi, Y., Song, X., Li, J., Wang, G., YuLong, F., & Geng, L. (2019). Analysis for effects of complex fracture network geometries on heat extraction efficiency of a multilateral-well enhanced geothermal system. *Applied Thermal Engineering*, *159*, 113828.

Siratovich, P., Sass, I., Homuth, S., & Bjornsson, A. (2011). Thermal Stimulation of Geothermal Reservoirs and Laboratory Investigation of Thermally Induced Fractures. *Transactions - Geothermal Resources Council*, *35*, 1529–1535.

Slatlem Vik, H., Salimzadeh, S., & Nick, H. M. (2018). Heat recovery from multiple-fracture enhanced geothermal systems: The effect of thermoelastic fracture interactions. *Renewable Energy*, *121*, 606–622.

Song, X., Guo, Y., Zhang, J., Sun, N., Shen, G., Chang, X., Yu, W., Tang, Z., Chen, W., Wei, W., Wang, L., Zhou, J., Li, X., Li, X., Zhou, J., & Xue, Z. (2019). Fracturing with Carbon Dioxide: From Microscopic Mechanism to Reservoir Application. *Joule*, *3*(8), 1913–1926.

Sowiżdżał, A., Machowski, G., Krzyżak, A., Puskarczyk, E., Krakowska-Madejska, P., & Chmielowska, A. (2022). Petrophysical evaluation of the Lower Permian formation as a potential reservoir for CO2-EGS-Case study from NW Poland. *Journal of Cleaner Production*, *379*, 134768.

Xie, J., Tonkin, R., Yeh, A., Wang, J., & O'Sullivan, M. (2025). Application of a geothermal wellbore simulator in evaluating an enhanced geothermal system. *Geothermics*, *125*, 103160.

Xue, Z. (2024). Machine learning based techno-economic assessment and optimization of an enhanced geothermal system. *Machine Learning*, *2024*, 06–21.

Xue, Z., & Chen, Z. (2023, March 10). *Deep Learning Based Production Prediction for an Enhanced Geothermal System (EGS)*. SPE Canadian Energy Technology Conference and Exhibition.

Xue, Z., Ma, H., & Chen, Z. (n.d.). *Numerical Investigation of Energy Production from an Enhanced Geothermal System Associated with CO2 Geological Sequestration*. SPE Western Regional Meeting.

Xue, Z., Ma, H., Sun, Z., Lu, C., & Chen, Z. (2024). Technical analysis of a novel economically mixed CO2-Water enhanced geothermal system. *Journal of Cleaner Production*, *448*, 141749.

Xue, Z., Ma, H., Wei, Y., Wu, W., Sun, Z., Chai, M., Zhang, C., & Chen, Z. (2024). Integrated technological and economic feasibility comparisons of enhanced geothermal systems associated with carbon storage. *Applied Energy*, *359*, 122757.

Xue, Z., Yao, S., Ma, H., Zhang, C., Zhang, K., & Chen, Z. (2023). Thermo-economic optimization of an enhanced geothermal system (EGS) based on machine learning and differential evolution algorithms. *Fuel*, *340*, 127569.

Xue, Z., Zhang, K., Zhang, C., Ma, H., & Chen, Z. (2023). Comparative data-driven enhanced geothermal systems forecasting models: A case study of Qiabuqia field in China. *Energy*, *280*, 128255.

Xue, Z., Zhang, Y., Ma, H., Lu, Y., Zhang, K., Wei, Y., Yang, S., Wang, M., Chai, M., Sun, Z., Deng, P., & Chen, Z. (2024). A Combined Neural Network Forecasting Approach for CO2-Enhanced Shale Gas Recovery. *SPE Journal*, *29*(08), 4459–4470.

Zhang, W., Wang, C., Guo, T., He, J., Zhang, L., Chen, S., & Qu, Z. (2021). Study on the cracking mechanism of hydraulic and supercritical CO2 fracturing in hot dry rock under thermal stress. *Energy*, *221*, 119886.